10-22-2008

Polymeric PARACEST Agents for Enhancing MRI Contrast Sensitivity

Yunkou Wu
University of Texas at Dallas

Youfu Zhou
University of Texas at Dallas

Olivier Quari
University of Texas at Dallas

Mark Woods
Portland State University, mark.woods@pdx.edu

Piyu Zhao
University of Texas at Dallas

See next page for additional authors

Citation Details

Wu, Y., Zhou, Y., Ouari, O., Woods, M., Zhao, P., Soesbe, T. C., ... & Sherry, A. D. (2008). Polymeric PARACEST agents for enhancing MRI contrast sensitivity. Journal of the American Chemical Society, 130(42), 13854-13855.

Authors

Yunkou Wu, Youfu Zhou, Olivier Quari, Mark Woods, Piyu Zhao, Todd B. Soesbe, Garry Kiefer, and A. Dean Sherry

Published in final edited form as:
J Am Chem Soc. 2008 October 22; 130(42): 13854–13855. doi:10.1021/ja805775u.

Polymeric PARACEST Agents for Enhancing MRI Contrast Sensitivity

Yunkou Wu[†], **Youfu Zhou**[†], **Olivier Quari**[†], **Mark Woods**[†], **Piyu Zhao**[†], **Todd C. Soesbe**[⊥], **Garry E. Kiefer**[†,‡], and **A. Dean Sherry**[*,†,⊥]
Department of Chemistry, University of Texas at Dallas, P.O. Box 830668, Richardson, Texas 75083, Macrocyclics, Inc., 2110 Research Row, Suite 425, Dallas, Texas 75235, and Advanced Imaging Research Center, The University of Texas Southwestern Medical Center, 5323 Harry Hines Boulevard, Dallas, Texas 75390

Abstract

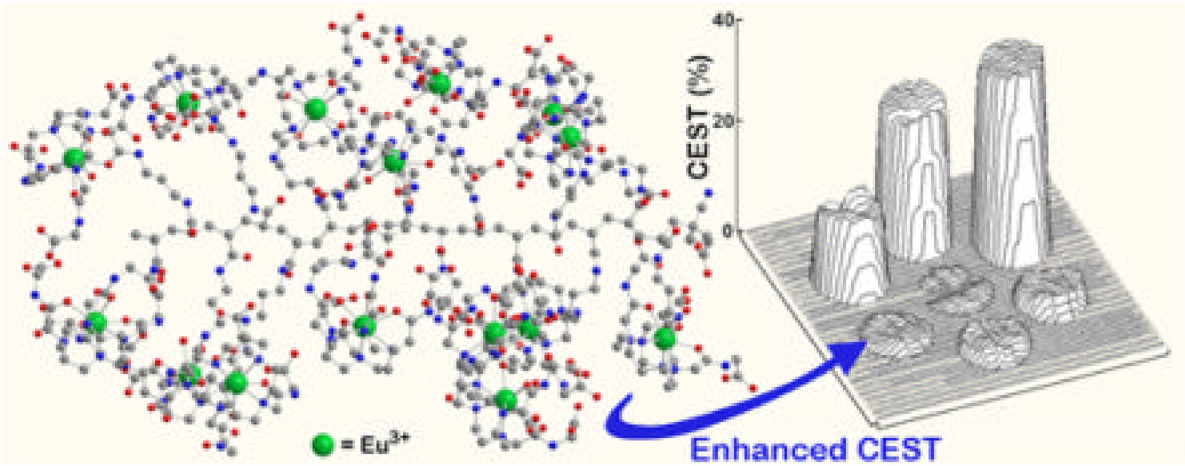

Linear polymers of PARACEST agents were prepared by using classical free radical chain polymerization conditions. The Eu^{3+}-polymers exhibited similar intermediate-to-slow water exchange and CEST characteristics as the Eu^{3+}-monomers. This provided an avenue to lower the detection limit of these imaging agents substantially and makes them potentially useful as MRI sensors for molecular imaging.

Magnetic resonance imaging (MRI) is an important clinical tool for anatomical imaging and monitoring certain tissue characteristics, such as perfusion and diffusion. Although MRI contrast agents are often used to improve diagnostic specificity, MRI is limited in molecular imaging applications because of its inherently low sensitivity when compared to nuclear medicine or fluorescence imaging.[1] Consequently, the search for new agents that can be detected by MRI at much lower concentrations continues to be an active area of research. The most widely used contrast agents are low molecular weight Gd^{3+}-based complexes that shorten

E-mail: sherry@utdallas.edu; dean.sherry@utsouthwestern.edu;.
[†]University of Texas at Dallas.
[‡]Macrocyclics, Inc.
[⊥]University of Texas Southwestern Medical Center.

Supporting Information Available: CEST spectra; experimental details. This material is available free of charge via the Internet at http://pubs.acs.org.

the T_1 of bulk water protons.[2] The effective molecular sensitivity of these agents may be improved by attaching multiple Gd^{3+} chelates to dendrimers[3] or polymers,[4] or by incorporating them into nanoparticles.[5] This approach can enhance the molecular relaxivity of Gd^{3+} and also result in larger particles that exhibit prolonged blood circulation for molecular targeting to tumors or other sites of interest.[4]

A new mechanism for generating image contrast, chemical exchange saturation transfer or CEST,[6] is of interest for targeted imaging applications. One intriguing aspect of CEST is that the effect can be switched on and off depending on whether a frequency selective pre-saturation pulse is applied or not. This feature, not available with Gd^{3+} agents because they are always on, allows acquisition of pre- and post-contrast images to be acquired nearly simultaneously. Paramagnetic CEST (PARACEST) agents with chemical exchange groups shifted well away from the bulk water signal offer significant advantages over diamagnetic CEST agents in that faster exchange systems are operable.[7] Theory shows that the detection limit of a single PARACEST exchanging species with an optimal water exchange rate, chemical shift, and relaxation properties is comparable to a single Gd^{3+}-based T_1 agent.[7] However, molecular imaging often requires the detection of targets that are present in concentrations too low to be detected by an agent with a single paramagnetic center so finding ways to maximize the number of PARACEST exchanging species at a targeted site is an important goal for MRI to complete in the field of molecular imaging. Van Zijl and coworkers first demonstrated this in various diamagnetic polymers, such as polyamino acids and even single-stranded RNA.[8] This stimulated us to consider polymeric PARACEST agents prepared by a simple free-radical chain polymerization reaction as a way to lower the detection limit of such agents.

Ligand **1** (prepared as described in supplementary materials) was polymerized using either 2%, 5% or 10% (*w*/*w*) azo-bis(4-cyanovaleric acid) as initiator in H_2O at 70°C to afford water soluble, linear polymers differing in size only. After 48 hr, the products were purified by dialysis using a 3kD MW cut-off membrane and the weight-average molecular weight (M_w) and number-average molecular weight (M_n) of each poly**1** was determined by light scattering GPC (Table 1). All three polymers exhibited comparable polydispersities (~1.13). Ligand **2** and its polymers were obtained by saponification of ligand **1** or the corresponding poly**1**. The Eu^{3+} complexes of all six polymers were prepared by reaction with excess $Eu(OTf)_3$ in H_2O (pH 6). The Eu^{3+}-polymer complexes were purified by adding EDTA to sequester any free Eu^{3+} followed by dialysis (3 kD MWCO).

Given the low MW of these new polymers and the known renal clearance of even larger Gd-based dendrimers,[9] we anticipate that these polymers will be excreted intact via renal filtration. However, no *in vivo* experiments have been performed to date. High resolution ^{1}H NMR spectra of the Eu^{3+}-monomers and the Eu^{3+}-polymers and the corresponding CEST spectra reveal a strong CEST peak in the range 48–54 ppm, consistent with each Eu^{3+}-ligand in the monomers and in the polymers adopting a square antiprism coordination geometry. The CEST magnitude on a per Eu^{3+} basis is the essentially same in each polymer as for the corresponding monomer. A fit of the CEST spectra to a 3-pool exchange model afforded the water residence lifetimes for each species (Table 1), demonstrating that water exchange remains largely unaffected by formation of a polymer.

The CEST features of Eu-**2** and the three Eu-poly**2** samples were compared on a per agent basis (Fig. 2) and the lower detection limit of each system, based on the assumption that a 5% change is easily detected, was determined from these data (Table 1). The detection limits for the longer polymers are in the range 60–80 μM, approaching the levels required for targeted imaging applications. CEST images of the Eu-**2** and Eu-poly**2**(2%) at three agent concentrations were collected by subtracting a sat-on image (+55 ppm) from the sat-off image (−55 ppm) (Fig. 3). The advantage of modestly sized PARACEST polymers is apparent from these images; at equivalent agent concentrations, Eu-poly**2**(2%) afforded a ~10-fold improvement in sensitivity over Eu-**2** at 300 μM (35% change in water intensity *versus* 3% respectively). Given that 100 μM Eu-poly**2**(2%) showed a 13% change in water intensity by CEST imaging and that local environmental factors could further the increase sensitivity of a targeted agent,[10] the true DL of such a targeted agent will likely be well below the values reported in Table 1, perhaps in the low μM range.

In summary, a convenient methodology for the preparation of polymeric PARACEST agents has been developed. The sensitivity and detention limits of these agents increase with polymer size. This work demonstrates that it is possible to create polymeric PARACEST platforms of modest size with tuned water exchange characteristics for optimal CEST imaging applications.

Supplementary Material

Refer to Web version on PubMed Central for supplementary material.

Acknowledgments

We thank Drs. Jinming Gao and Xiaoyu Wang (UTSW) for their assistance with the light scattering GPC. Financial support from the National Institutes of Health (CA115531, RR02584 and EB04285) and the Robert A. Welch Foundation (AT-584) is gratefully acknowledged.

References

1. Weissleder R, Mahmood U. Radiology 2001;219(2):316–333. [PubMed: 11323453]
2. Caravan P, Ellison JJ, McMurry TJ, Lauffer RB. Chem Rev 1999;99(9):2293–2352. [PubMed: 11749483]
3. Kobayashi H, Brechbiel MW. Curr Pharm Biotechnol 2004;5(6):539–549. [PubMed: 15579043]
4. Kim JH, Park K, Nam HY, Lee S, Kim K, Kwon IC. Prog Polym Sci 2007;32(8–9):1031–1053.
5. Lanza GM, Winter PM, Caruthers SD, Morawski AM, Schmieder AH, Crowder KC, Wickline SA. J Nucl Cardiol 2004;11(6):733–743. [PubMed: 15592197]
6. Ward KM, Aletras AH, Balaban RS. J Magn Reson 2000;143(1):79–87. [PubMed: 10698648]
7. Woods M, Donald EWC, Sherry AD. Chem Soc Rev 2006;35(6):500–511. [PubMed: 16729144]
8. Zhou JY, van Zijl PCM. Prog Nucl Mag Res Sp 2006;48(2–3):109–136.
9. Kobayashi H, Brechbiel MW. Mol Imag 2003;2:1–10.Misselwitz B, Schmitt-Willich H, Ebert W, Frenzel T, Weinmann H-J. MAGMA 2001;12:128–134. [PubMed: 11390268]
10. Hanaoka K, Lubag AJM, Castillo-Muzquiz A, Kodadek T, Sherry AD. J Magn Reson Imag 2008;26:608–617.

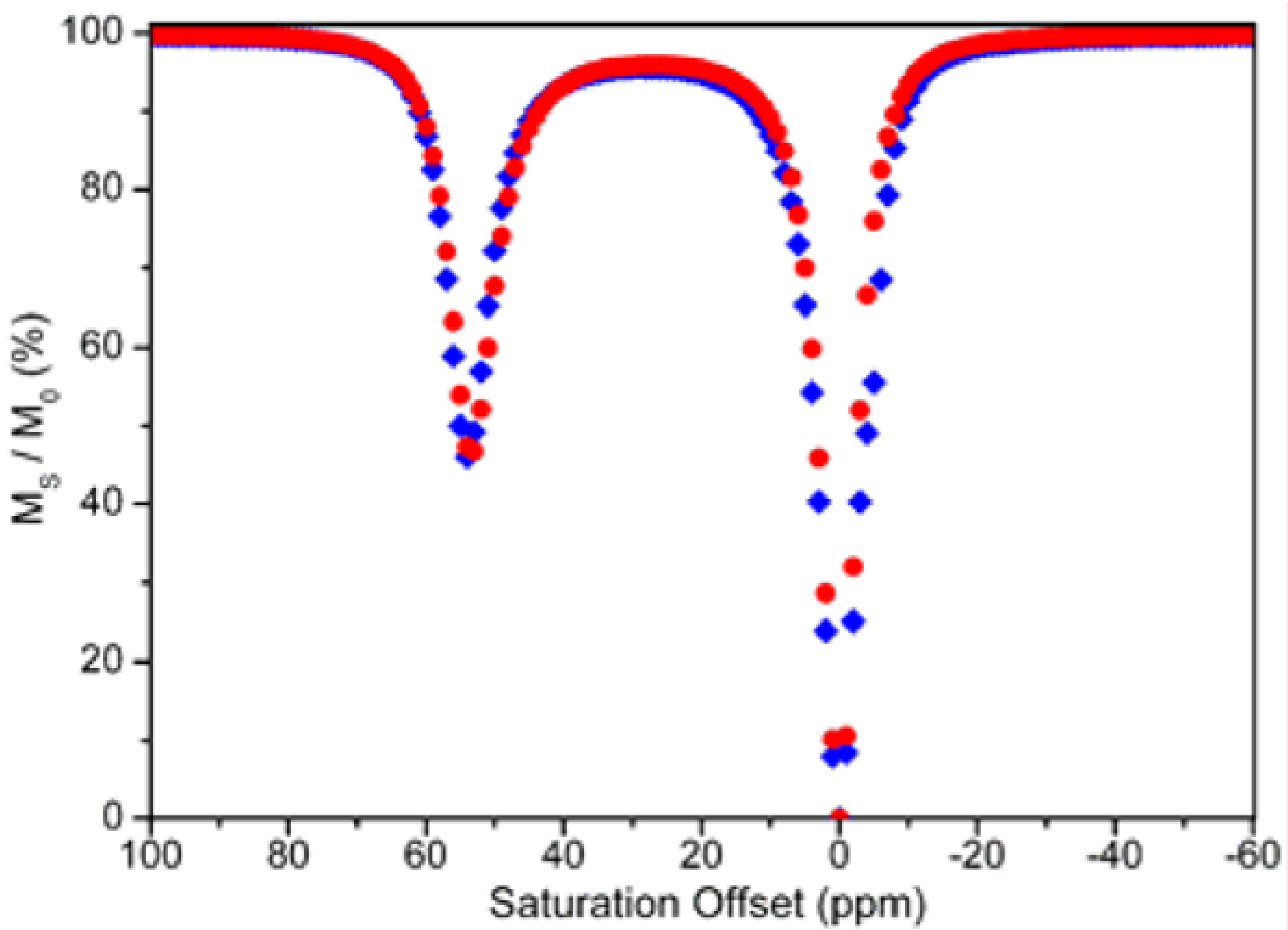

Figure 1.
CEST spectra of Eu-**2** (red) and Eu-poly**2**(2%) (blue) recorded at 11.75 T and 298 K. [Eu^{3+}] = 30 mM, B_1 = 14.1 μT, sat. time = 4 s.

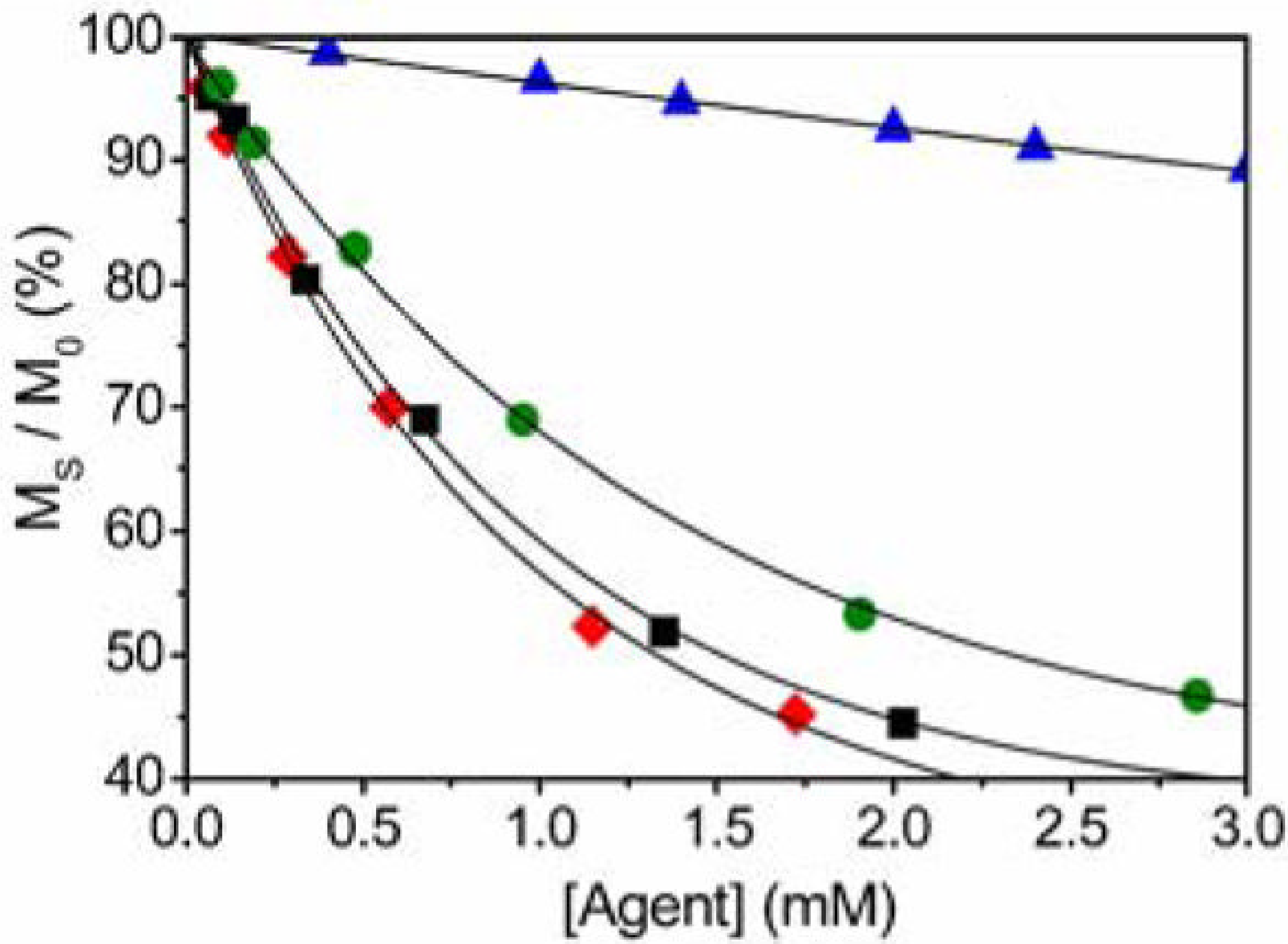

Figure 2.
Maximum CEST per [agent] of Eu-**2** (▲) and Eu-poly**2 (2% ◆**, **5% ■**, **10% ●)**, 11.75 T, 298 K, B_1 = 14.1 μT, sat. time = 4 s.

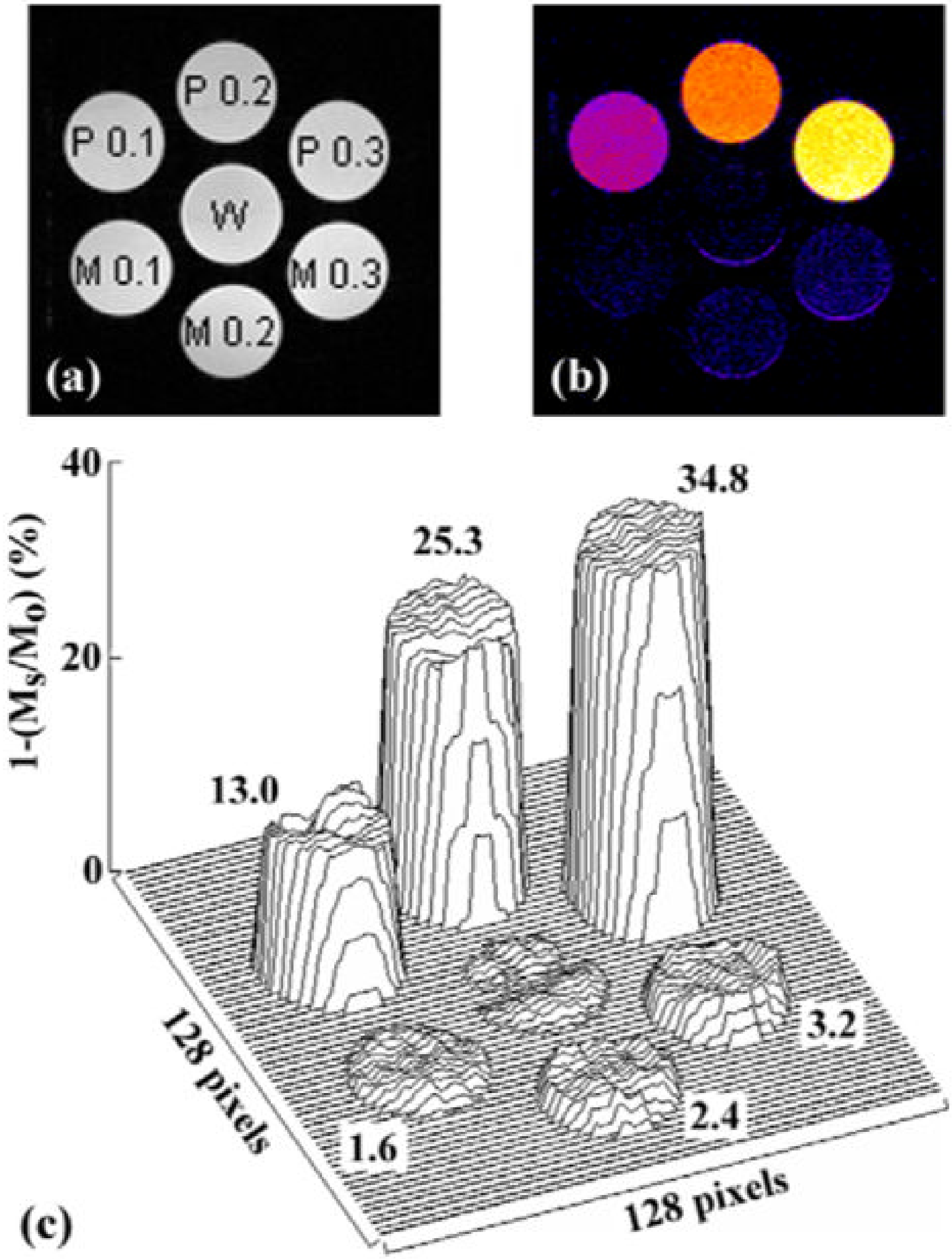

Figure 3.
CEST images of Eu-poly**2**(2%) and Eu-**2** phantoms at 9.4 T, 292 K. The agent concentrations (mM) are given for monomer, M, and polymers, P, in (a), W refers to water as control. (b) CEST images and (c) the corresponding 3D surface plots.

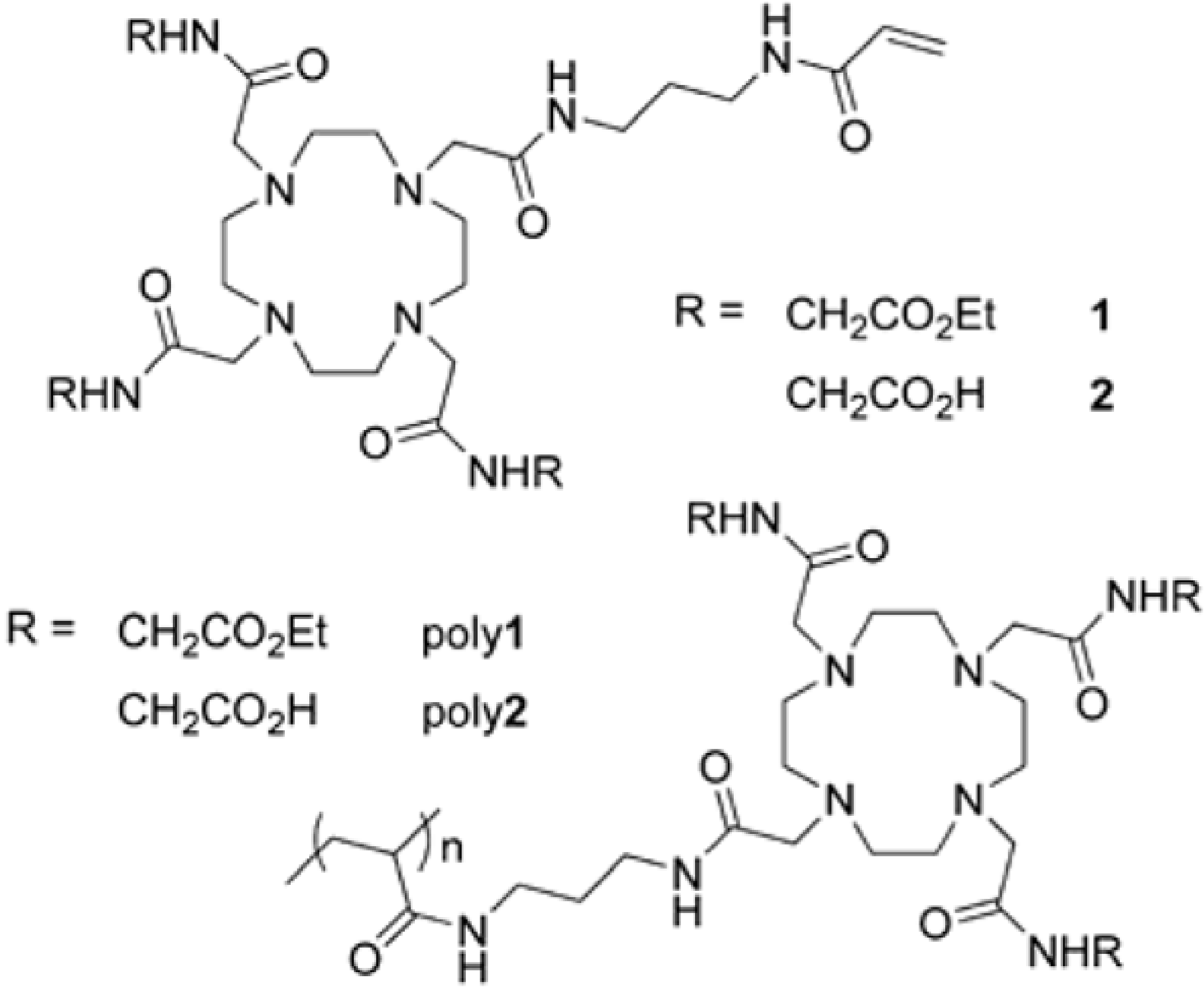

Chart 1.
The structures of the two monomers (top) synthesized in this work and the polymers (bottom) prepared from them.

Table 1

Selected properties of polymers derived from Eu-**1** and Eu-**2**.

	Initiator	Mw	Mw/Mn[a]	DP[b]		τ_M (ms)	5% DL[c] (μM)
1	-		-	-	Eu-**1**	0.221 ± 0.016	1650 ± 160
poly**1**	2%	13400	1.149	17.4	Eu-poly**1**	0.201 ± 0.008	65 ± 6
poly**1**	5%	11500	1.130	14.8	Eu-poly**1**	0.189 ± 0.014	84 ± 2
poly**1**	10%	8100	1.128	10.5	Eu-poly**1**	0.186 ± 0.015	130 ± 6
2	-		-	-	Eu-**2**	0.144 ± 0.007	1365 ± 25
poly**2**	2%	-	-	17.4[d]	Eu-poly**2**	0.160 ± 0.008	71 ± 4
poly**2**	5%	-	-	14.8[d]	Eu-poly**2**	0.162 ± 0.005	82 ± 7
poly**2**	10%	-	-	10.5[d]	Eu-poly**2**	0.151 ± 0.007	117 ± 7

[a] polydispersity,

[b] degree of polymerization,

[c] detection limit,

[d] degrees of polymerization are the same as for the corresponding poly**1**